Supplemental material for Photonic Berry curvature in double liquid crystal microcavities with broken inversion symmetry

P. Kokhanchik,[1] H. Sigurdsson,[1,2] B. Piętka,[3] J. Szczytko,[3] and P.G. Lagoudakis[1,2,*]

[1]*Skolkovo Institute of Science and Technology, Bolshoy Boulevard 30, bld. 1, Moscow, 121205, Russia*
[2]*School of Physics and Astronomy, University of Southampton, Southampton SO17 1BJ, United Kingdom*
[3]*Institute of Experimental Physics, Faculty of Physics, University of Warsaw, ul. Pasteura 5, PL-02-093 Warsaw, Poland*

(Dated: February 12, 2021)

TRANSMITTED STOKES PARAMETERS AND FIELD DISTRIBUTION FROM THE DOUBLE CAVITY

The Stokes parameters of the transmitted/reflected cavity light $|\Psi\rangle = (\psi_+, \psi_-)^t$ are written in the circular polarization basis as follows, linear vertical-horizontal projection $S_1 = \mathrm{Re}(\psi_+\psi_-^*)$, linear diagonal-antidiagonal projection $S_2 = -\mathrm{Im}(\psi_+\psi_-^*)$, right-hand and left-hand circular projection $S_3 = (|\psi_+|^2 - |\psi_-|^2)/2$, and total light intensity $S = (|\psi_+|^2 + |\psi_-|^2)/2$. Figures S1 and S2 show the transmitted Stokes parameter distribution and the electric field distribution in reciprocal space, respectively, where we excite at the energy in the second band from the bottom corresponding to maximum Berry curvature [see Fig. 2(c) in main manuscript] (i.e., at $E = 1.6603$ eV). We use reciprocal space to present our calculations as they are performed using the Berreman method. Figure S3 correspond to transmitted Stokes parameter distribution depending on k_y and energy. We present the distributions for the case of an isolated TE-TM + XY cavity (see Figs. S1 to S3 upper rows), an isolated Rashba-Dresselhaus cavity (see Figs. S1 to S3 middle rows), and for the two coupled cavities (see Figs. S1 to S3 bottom rows).

The top row in Fig. S1 shows the expected polarization pattern of a TE-TM + XY system. Two shifted parabolas of different effective masses whose energies correspond to rotating linear polarization eigenmodes as dictated by the effective magnetic field shown in Fig. 1(c) in the main manuscript. The middle row shows the dominant transmission coming from circularly polarized states [see Fig. S1(f)] corresponding to the two momentum displaced valleys of the Rashba-Dresselhaus Hamiltonian. We point out that additional finite Stokes parameters appearing in Fig. S1(c) and Figs. S1(d,e) are due to both finite reflectivity of the modelled cavity and higher order contributions to the cavity mode mixing (see Ref. [1]).

In the third row of Fig. S1 the two coupled cavities result in a nontrivial polarization texture emerging from all four bands in the system. The different amount of transmission across the bands in both frequency and momentum for our chosen incident diagonally polarized light makes analysis quite challenging. Indeed, the spin degree of freedom is entangled with the cavity degree of freedom through the parameter J in Eq. (5) which forbids us from analysing the system in the framework of two uncoupled pseudospins. As such, the definition of a band's polarization through the isomorphic relation between the SU(2) and the SO(3) group is lost. None-the-less, the Berreman calculations allow one to characterize the transmitted polarization of the cavity with great detail which becomes a useful tool when comparing theory with experiment.

QUANTUM GEOMETRIC TENSOR COMPONENTS AND BERRY CURVATURE OF ALL BANDS

Figure S4 shows the QGT components (see labels in each panel) in the remaining bands $n = 1,3,4$ with band $n = 2$ shown in Fig. 2 in the main manuscript.

* p.lagoudakis@skoltech.ru

[1] K. Rechcińska, M. Król, R. Mazur, P. Morawiak, R. Mirek, K. Łempicka, W. Bardyszewski, M. Matuszewski, P. Kula, W. Piecek, P. G. Lagoudakis, B. Piętka, and J. Szczytko, Engineering spin-orbit synthetic hamiltonians in liquid-crystal optical cavities, Science **366**, 727 (2019).

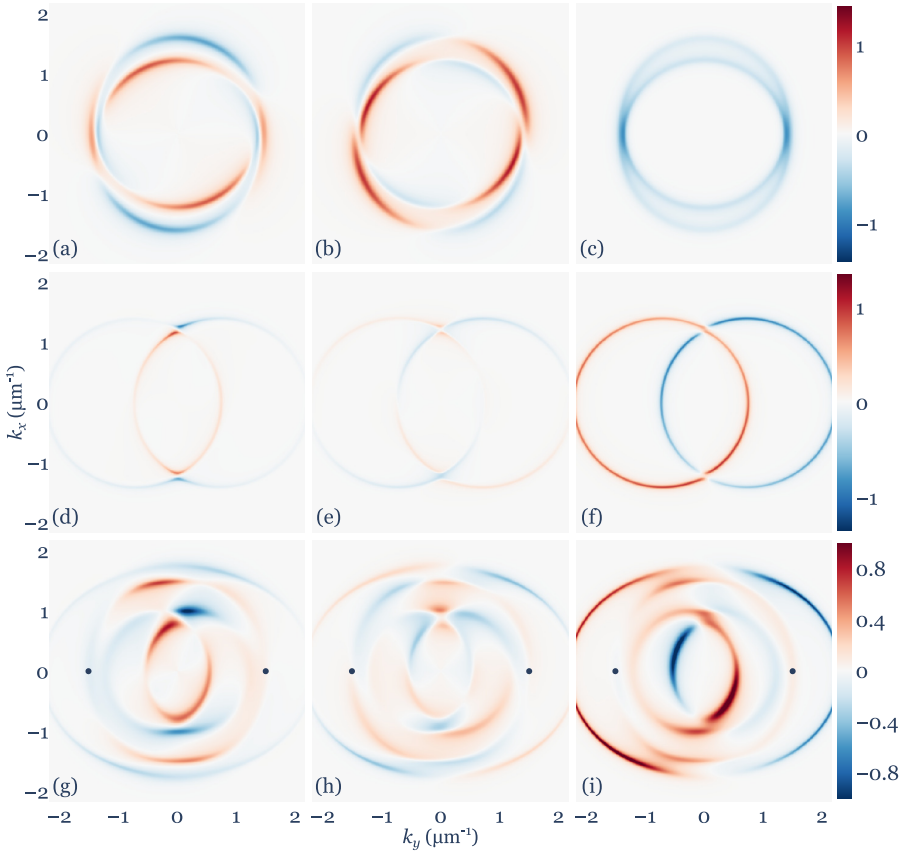

FIG. S1. **Stokes parameters of the transmitted cavity light in reciprocal space.** The incident light is diagonally polarized. Calculations were performed using the Berreman method. Panels from left to right correspond to S_1, S_2 and S_3 respectively. Top row shows the isolated TE-TM + XY system, the middle row shows the isolated RD system, and the bottom row shows the two coupled systems. The energy $E = 1.6603$ eV is the same for all figures and is chosen resonant with the second lowest band point of maximum Berry curvature. Black dots in (g,h,i) shows the position of the Berry curvature extremum.

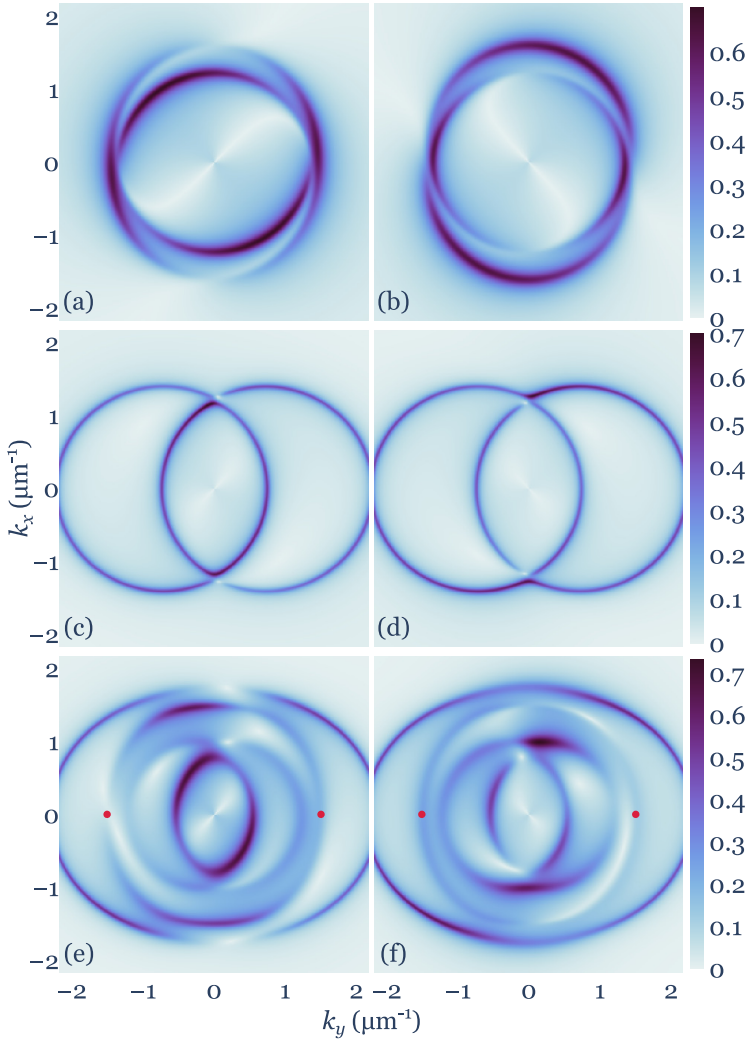

FIG. S2. **Amplitudes of the transmitted electrical field components along x ($|\psi_x|$, left column) and y ($|\psi_y|$, right column) axes normalized to the incident light electrical field amplitude.** Calculations were performed using the Berreman method. Analogous to the order in Fig. S1 we show the field amplitudes for (a,b) isolated TE-TM + XY system, (c,d) isolated RD system, (e,f) coupled systems. Red dots in (e,f) shows the position of the Berry curvature extremum.

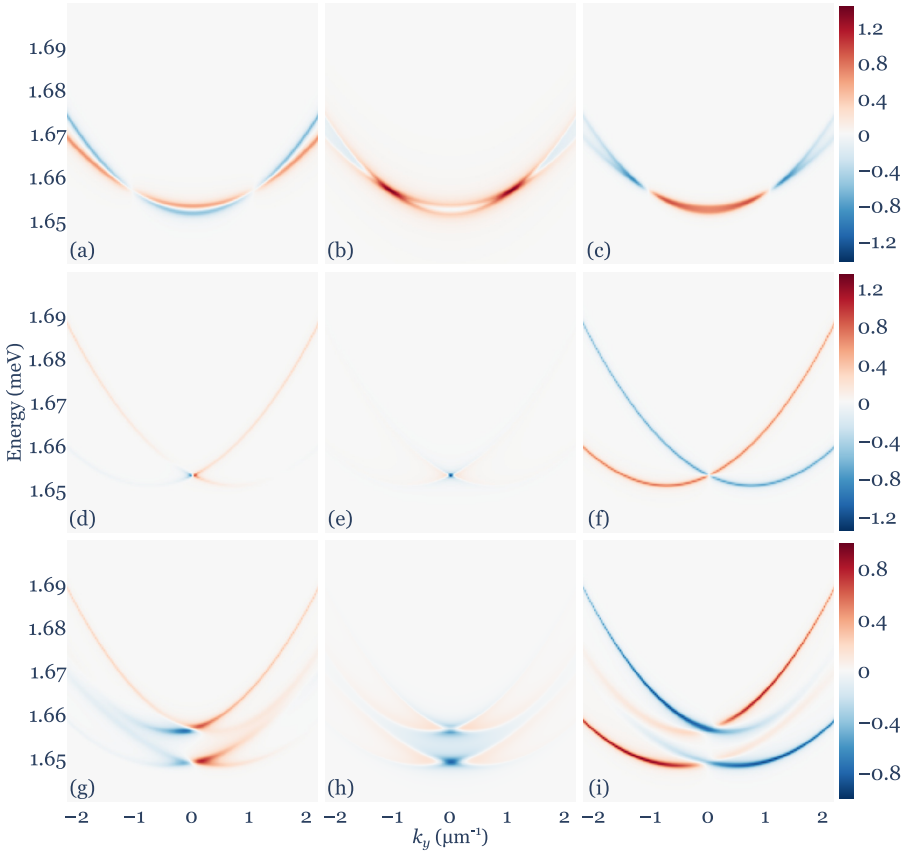

FIG. S3. **Stokes parameters of the transmitted cavity light depending on k_y and energy.** The incident light is diagonally polarized. Calculations were performed using the Berreman method at $k_x = 0$. Panels from left to right correspond to S_1, S_2 and S_3 respectively. Top row shows the isolated TE-TM + XY system, the middle row shows the isolated RD system, and the bottom row shows the two coupled systems.

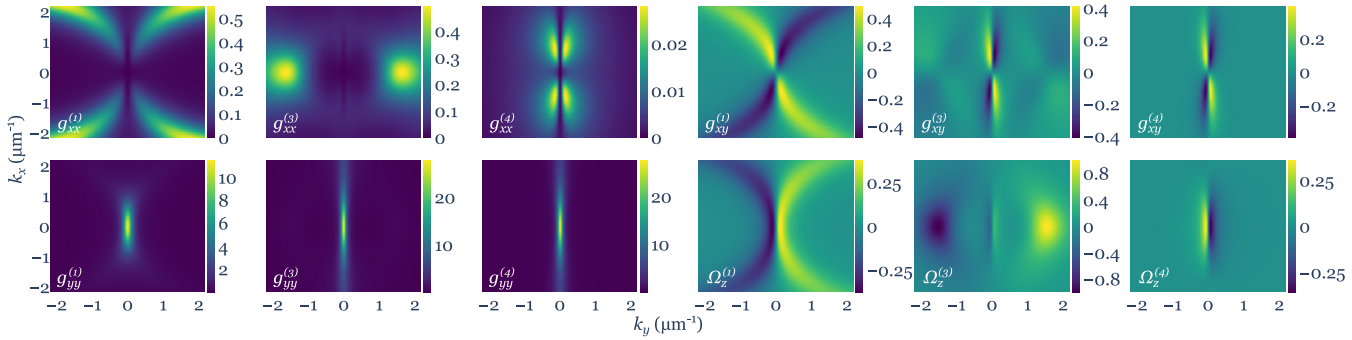

FIG. S4. **Quantum geometric tensor components and Berry curvature.** The quantum geometric tensor components $g_{ij}^{(n)}$ and the Berry curvature $\Omega_z^{(n)}$ for bands $n = 1, 3, 4$ (counted from lowest energy band to highest).